



## Removal of E102 dye from aqueous solution by adsorption on the surface of polyaniline walnut husks nanocomposite.

Shurooq S. Kadhium , Asmaa J. AL-Lamei , Nagham Majed

Chemistry Department, College of Science, Al-Mustansiriyah University, Iraq



CrossMark

### Abstract

Development of a new, cheap, efficient, and ecofriendly adsorbents become important demand for the treatment of waste water, so nano polyaniline walnut husks is considered a good choice. A sample of nanocomposite was prepared from polyaniline. The prepared sample was characterized using various characterization techniques such as FT-IR, SEM and XRD analysis. The SEM analysis of sample shows nanostructures with pore ranging (2-100 nm). The adsorptive properties of this sample were examined by eliminating E102 dye from aqueous solution. Amount Experimental methods were performed at room temperature (25°C) to study the different variables which affect the adsorption process like: nanocomposite amount, initial concentration of dye, and contact time. The experimental results at equilibrium were determined using Langmuir and Freundlich adsorption isotherms and show best fitted with Langmuir model which reveal that the adsorption of E102 dye by the nanocomposite is monolayer adsorption. Kinetics aspects was also investigated by evaluating parameters from pseudo- first and pseudo-second order reaction equations on adsorption rate which show good fitting with both kinetics equations, but pseudo-second order equation was the best to describe the kinetics parameters.

**Keywords:** E102, langmuir models, Nanocomposite, polyaniline walnut husks.

### 1. Introduction

Nano-adsorbents are known as materials with dimensions of less than 100 nm. Adsorbents can be categorized as agricultural, inorganic, polymeric and composite residues into four types based on their source. With the development of industrial, commercial and agricultural fields as well as with the improvement in pharmaceutical and medical science, this technology is rapidly enhanced. The chemical structures of the adsorbents play an important role in the phenomenon of adsorption. Adsorbents containing chelating groups, such as amine, amide, oxime, hydroxyl, thiol, carboxyl, etc., are strong candidates for removing contaminants.

In recent decades, in terms of their vast surface area, polymeric adsorbents have appeared as potential alternatives to traditional adsorbents, and polymeric

materials can often adsorb many pollutants effectively. Because of its environmental stability, polyaniline is one of the most interesting polymers to conduct[1]. In practice, Polyaniline can be prepared via chemical or electro-chemical oxidation of aniline in acidic medium [2, 3]. These dyes will be more stable and harder to biodegrade due to the complex aromatic molecular structure of dyes [4, 2]. Chemical precipitation, adsorption, ion exchange, biodegradation, membrane filtration, coagulation, flocculation, etc. are the basic technologies used to treat dye-containing effluents. Adsorption is commonly used and most flexible, as other techniques have high capital costs and low efficiency[3,5]. Strong environmental performance due to its high electrical conductivity. Adsorption is commonly used and is the most flexible, as other techniques have high cost of capital and low

\*Corresponding author e-mail.: [asas.jameil@uomustansiriyah.edu.iq](mailto:asas.jameil@uomustansiriyah.edu.iq)

Receive Date: 31 October 2020, Revise Date: 04 March 2021, Accept Date: 21 April 2021

DOI: 10.21608/EJCHEM.2021.47440.2987

©2021 National Information and Documentation Center (NIDOC)

efficiency[3,5]. Due to its high electrical conductivity, strong environmental stability and ease of preparation [6], polymers, polyaniline (PAn) is unique. A colored us can mainly be referred to as dye. Dye may generally be referred to as a colored material with an affinity to the substrate to which it is used[7]. Dyes have an aromatic molecular structure that is likely to come from hydrocarbons such as toluene, benzene, anthracene, naphthalene, xylene. Low-cost waste precursors such as walnut [8] or hazelnut shells [9], sunflower seed hulls [10], sawdust [11], fruit peels [12]. may be used for activated carbon production and they become good adsorbents for the reduction of COD or other pollutants in wastewaters. In addition, polymers such as polyaniline and polypyrrole are used to enhance the sorption characteristics of certain materials [13,14,15] as a modification compound.

Nanotechnology is preferred in the area of water purification because it offers the possibility of an efficient method for water treatment and removal of pollutants and germs from wastewater. Contamination of water resources to dye pollutants is thought-about as an environmental important problem. Thousands types of dyes have been used in various fields such as the textiles, paper, printing, paints, plastics, cosmetics and leather industries, and food technology industries [16]. These dyes are carcinogenic in nature and contaminate the surface and ground water, thereby, making it unfit for irrigation and drinking. Large number treatment techniques have been used for removing dyes from aqueous solution like photodegradation [17] membrane filtration [18], ion exchange [19], electrochemical and adsorption processes [20]. Due to its high efficiency, low cost and simple to operate, adsorption is considered an attractive treatment to remove dyes from water .

A new sample of nanocomposite was prepared, characterized and used in this work to research the effective behavior of aqueous solution adsorption of E102 dye. In order to achieve the best conditions for the adsorption process , different variables such as nanocomposite dosage, contact time and the effect of the initial concentration of E102 dye were examined. In addition, using the Freundlich and Langmuir equations, thermodynamic adsorption parameters were determined.

## 2. Experimental

### 2.1. Materials

Aniline (PARK) which was used after double distillation, E102 dye was supplied by Aldrich USA Sigma Chemical ( $C_{16}H_9N_4Na_3O_9S_2$ ) Mwt. = 534.4g  $mol^{-1}$  and HCl (36%) , $(NH_4)_2S_2O_8$  were supplied by BDH Chemicals LTD.

### 2.2. Instrumentals

Fourier Transform Infrared Spectrophotometer (FT-IR): SHIMADZU (IR-PRESTIGE 21). Scanning electron microscope (SEM) : Bruker Nano GmbH, Germany. x-ray Shimadzu -6000.

### 2.3. Synthesis Procedure of nanocomposite:

Aniline was purified before use. The walnut shell (WS) was washed and drained, and sifted through a sieve of 150  $\mu m$ . The monomer solution was made by applying (0.05mol) aniline (sp. Gel.02gm / ml) to 10ml of 1 M HCl (12gm) WS to the aniline hydrochloride solution and swirling constantly in the ice bath. oxidizing agent  $(NH_4)_2S_2O_8$  (0.05mole) was added slowly to start the polymerization. After completion of polymerization the color of solution turned green. For 5 hours, the solvent was mixed on a magnetic stirrer. The mixture was left at around 4-6°C overnight. The substance was purified and washed repeatedly with 1 M HCl accompanied by acetone, ethanol and deionized water, dried in the oven at 50°C and distinguished by powder.

### 2.4. Adsorption Procedure

Series of E102 dye concentrations (20-120 mg/L) were prepared from stock solution (1000 ppm) and the calibration curve was establish at  $\lambda_{max} = 426$  nm. Adsorption experiments were duplicate and carried out by taking 50 mL from each concentration of E102 (20-120 mg/L) in 250 mL conical flask with 0.08 g of nanocomposite and placed in a thermostatic shaker water bath (Julabo SW23) at 25°C. Every 10 min interval, 5mL from each flask was withdrawn and filtered to measure the UV-Visible absorbance of dye at the maximum wavelength 426nm. The average of the results was taken to calculate the concentration of E102 dye in all experiments. The amount of dye adsorbed at equilibrium  $q_e$  (mg/g) was determined according to the following equation:

$$q_e = (C_0 - C_e) V / w \quad \text{----- (1)}$$

Where  $C_0$  and  $C_e$  are the concentration of E102 (mg/L) at initial and at equilibrium stage respectively,  $V$  is the volume of solution (L),  $w$  is the weight of nanocomposite (g).

### 3. Results and Discussion

#### 3.1. Characterization of Nanocomposite Sample

##### 3.1.1. FTIR Spectra

Table (1) and Fig. 1 shows the FTIR spectra of PAN/WS composites, in comparison with that of pure PAN, at 600- 4,000 $\text{cm}^{-1}$ . The band at 1288.94 $\text{cm}^{-1}$  belongs to the C-N stretching of a secondary aromatic amine strengthened by protonation of PAN, and is also present in spectra of composite. Peaks at 1558.54 and 1489.10  $\text{cm}^{-1}$  corresponding to quinone and benzene slightly shifted ring-stretching deformations of PAN are also detected in the nanocomposite. Furthermore, the characteristic peaks of PAN are seen at 2926 -3240.52  $\text{cm}^{-1}$  (aromatic C-H stretching) and 802.41  $\text{cm}^{-1}$  (out-of-plane deformations of C-H) [21]. These peaks can also be seen in the spectra of PAN/WS composites. All bands in composites are slightly shifted, which indicates that there is some interaction between PAN and WS.

Table 1: Characteristic absorption peaks obtained from FTIR spectrum of PAN and PAN-WS nanocomposite.

Wave number ( $\text{cm}^{-1}$ )	functionality
515-595	C-N-C bonding mode of aromatic ring
622-750	C-C,C-H bonding mode of aromatic ring
802.41	C-H out of plane bonding in benzenoid ring
1558.54-1489.10	C-N stretching of benzenoid ring
1558.4	C=N Stretching of quinoid ring
2800-3000	Symmetric stretch vibration band of methylene[-(CH <sub>2</sub> ) <sub>n</sub> -] and methyl-(CH <sub>3</sub> )

##### 3.1.2. XRD analysis

To examine the structure of the nanocomposites PAN and PAN-WS, XRD research was used. The standard XRD patterns for PAN and PAN-WS nanocomposites as seen in Fig (2). The PAN peak diffracted with a d spacing of 4.593 Å and 3.461 Å at an angle of  $2\theta = 19.31^\circ$  and  $2\theta = 25.72^\circ$ , respectively. As is apparent in PAN and its nanocomposites, due to the polymer (PAN) chain's coordinate and perpendicular periodicity, large diffraction peaks occur between  $10^\circ$  and  $20^\circ$ . In the XRD pattern which shows low crystallinity of the conductive polymers due to recurrence of benzenoid and quinoid rings in PAN chains [22]; moreover, PANI crystal size, D, is 4.4 nm which was calculated by Scherrer's equation [21]. crystal size of nanocomposites increased from 4.4 nm for PAN to 7.4 nm for PAN-WS. It can be seen that the XRD

patterns of nanocomposites are similar to that of PAN. According to Fig. 2, in the given range recorded for the broad peak, two distinct sharp peaks at  $2\theta=19.31^\circ$  and  $2\theta=25.72^\circ$  with planes of (010) and (200), respectively.

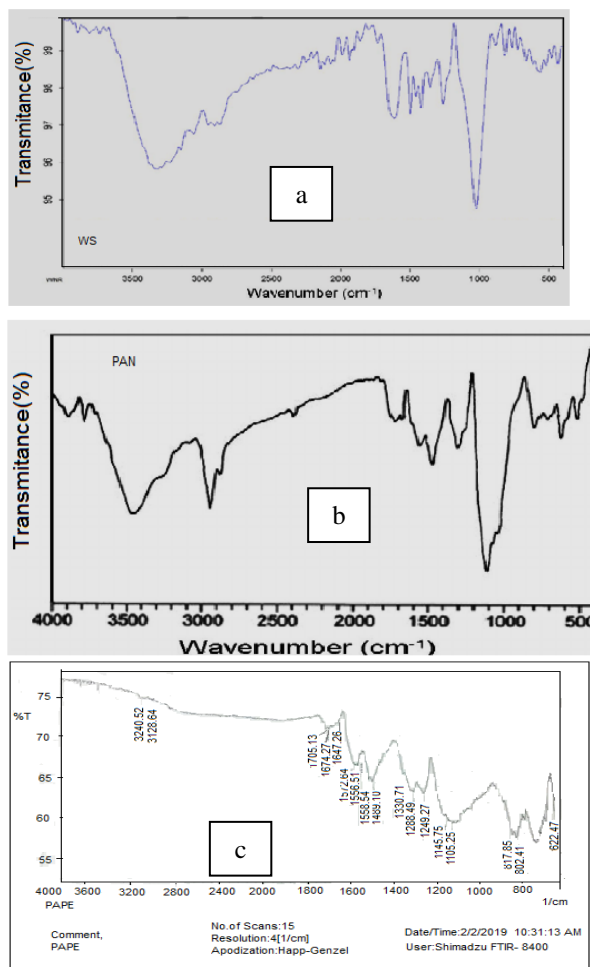


Fig. 1. FTIR for (a) walnut husks, (b) pure PAN, (c) PAN-WS nanocomposite

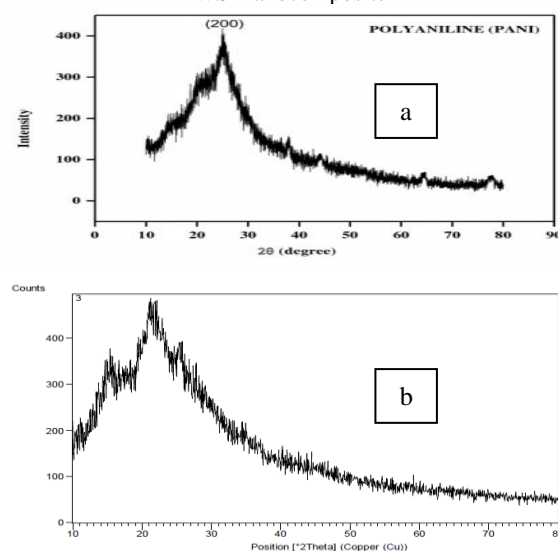


Fig. 2. (a) XRD for polyaniline only, (b) XRD for nanocomposite (PAN/WS)

### 3.1.3. SEM analysis

The surface microstructure of nanocomposite was studied with scanning electron microscope (SEM) 1 which provides the information about the size and shape of the particle and pore. The SEM photographs of nanocomposite and walnut shell are shown in (Fig. 3a and 3b) and reveal that the sample consists of small and big grain. Is irregular.

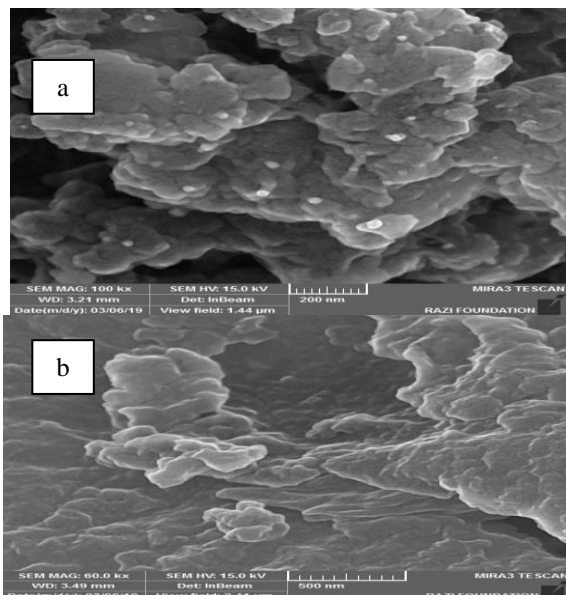


Fig. 3 . SEM for (a) nanocomposite (b)walnut husks

## 3.2. Adsorption Study

### 3.2.1. Effect of Nanocomposite dosage

In order to study the effect of adsorbent dosage on adsorption process, different amount of nanocomposite (0.01,0.02,0.04,0.06,0.08 and 0.1 g) per 50 mL of solution were examined at 25°C and 40mg/L as initial concentration of dye. The percentage removal of E102 dye was calculated according the following equation:

$$\% \text{ Removal} = (C_0 - C_e) / C_0 \times 100 \quad \text{-----(2)}$$

(Fig. 4) show the results of dye removal and reveal that the amount of E102 dye adsorbed increased with increasing the adsorbent dosage and reached a maximum value at 0.08 g /50 ml of solution. When the dosage was 0.1 g of nanocomposite, decreasing in the percentage removal of E102 was noticed. This is may be due to increase the adsorption sites which lead to the unsaturation of these sites during adsorption process [14,23].

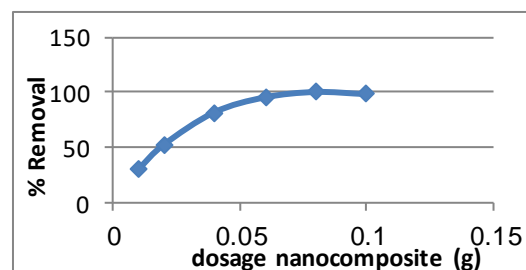


Fig. 4. Effect of Nanocomposite dosage on adsorption of E102 dye

### 3.2.2. Effect of contact time and initial concentration on the adsorption process

Impact on the adsorption mechanism of contact time and initial concentration at 25 °C, the influence of contact time was analyzed using the initial concentration range of E102 dye (20-120) mg / L over various time periods. Table ( 2) reveals that the percentage of E102 dye elimination has declined with an increase in the original E102 dye concentration. Despite the percent of adsorption has decreased with the increase in initial dye concentration, The certain amount of dye adsorbed per unit mass of adsorbent has increased with increase in dye concentration. The increase in initial dye concentration causes an increase in the interaction between dye molecules and nanocomposite surface. From (fig. 5) we can see that the removal was increased rapidly during the first hour of adsorption process, and then it slow down with the increase in contact time. The time necessary to reach the equilibrium for the removal of the E102 molecules at different concentrations by nanocomposite was established to be 60 min.

Table 2 : The effects of the initial dye concentration on the adsorption process.

Initial dye concentration (mg/L)	% Removal efficiency
20	99.8
40	99.1
60	93.17
80	78.46
100	71.26
120	62.41

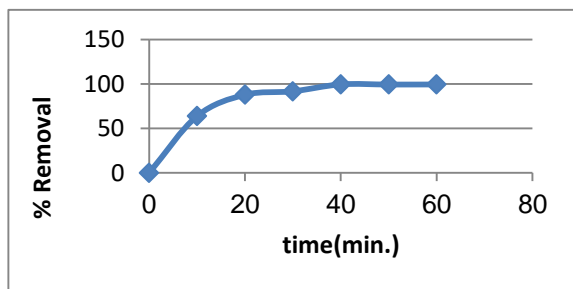


Fig. 5 . The effects of the contact time on the adsorption process.

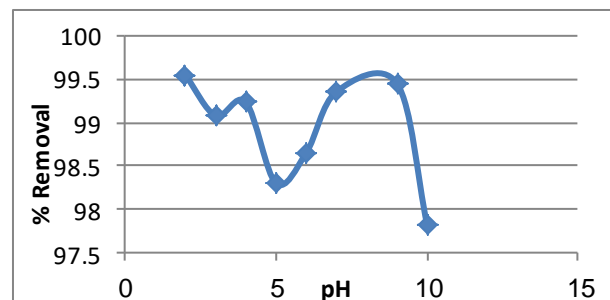


Fig 7 .Effect of pH on % removal of E102 dye on PAN/WS adsorbent.

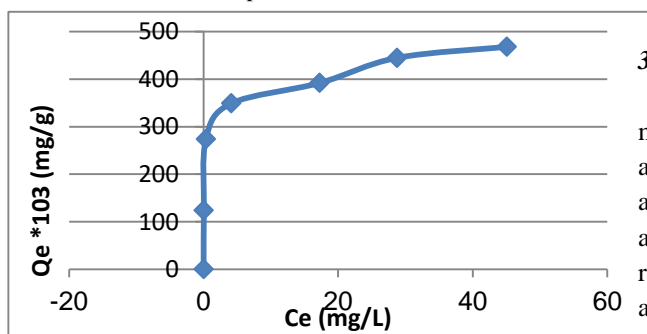


Fig 6 . Effect of different concentration on removal of E102 dye at equilibrium at 25°C

Also, the effect of initial concentration of E102 dye (20-120 mg/L) was shown in (Fig. 6) and revealed that the amount adsorbed of E102 dye increases with increasing initial concentration, so the removal of E102 depends on the concentration of the dye. At low concentration, the active adsorption sites are relatively high so E102 dye molecules can easily find the accessible adsorption sites, but at higher concentrations the available site of adsorption decreasing with more time. In addition, at high concentration E102 dye molecules have ability to aggregate in aqueous media under different shapes and sizes [24]. These aggregations may be preventing easily accessible of E102 dye molecules in vacant sites of adsorbent.

### 3.2.3. pH effects

In evaluating the substantial adsorption potential of an adsorbent, pH plays an important role.

The variance of the percent adsorption of E102 dye on PAN/WS adsorbents versus pH (2-10) is discussed in this study.

Figure 7 shows all the outcomes of this analysis. It is observed that with increased pH from 2 to 10, percent elimination decreases from 99.5 to 97.8 percent., the electrostatic repulsion between the surface of the adsorbent, negatively charged, and the anionic dye reduces the adsorption capacity and removal of coloring.

### 3.3. Adsorption Isotherms of Process

Adsorption isotherms have characterized the mechanisms, surface properties and the closeness of adsorbent towards adsorbate. The outcomes of the adsorption equilibrium are conveniently defined by adsorption isotherms, which are identical to the relationship between the adsorbed solute mass per adsorbent unit mass ( $q_e$ ) and the equilibrium solution concentration ( $C_e$ ). Experimental adsorption data must be integrated into a suitable isothermal model. Thus, the most widely known, Langmuir and Freundlich isotherms, were used to evaluate the relationship between the amount of dye adsorbed and the remained concentration of dye at equilibrium. Langmuir isotherm [17] assumes homogeneous monolayer adsorption on the surface of adsorbent which contains finite number of sites, so no further adsorption may take place on these sites, the linear form of Langmuir equation can be written as follow:

$$\frac{C_{eq}}{q_{eq}} = \frac{1}{K_L q_{max}} + \frac{1}{q_{max}} C_{eq} \quad \text{----- (3)}$$

where  $C_{eq}$  is the equilibrium concentration of the dye (mg/L),  $q_{eq}$  is the amount of adsorbate dye per each gram of composite at equilibrium,  $q_{max}$  (mg/g) is the maximum amount of adsorbed dye corresponding to complete monolayer coverage,  $K_L$ (L/mg) is the Langmuir adsorption equilibrium constant related to the energy of adsorption. The Langmuir constants can be evaluated from the slope and the intercept of the linear equation. (Fig.8) represents applying of Langmuir isotherm equation on experimental results of adsorption of E102 dye on Nanocomposite adsorbent.

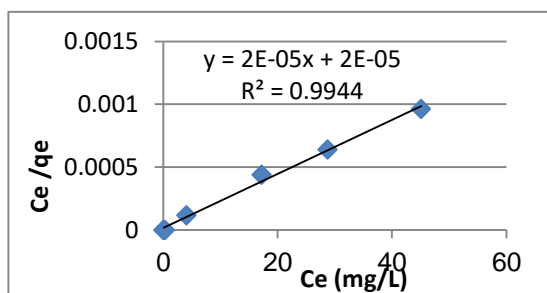


Fig 8 . Langmuir isotherm for adsorption of E102 dye on to Nanocomposite surface.

Freundlich isotherm [18] model is derived from Langmuir isotherm and assumes a heterogeneous surface of adsorption capacity and can be applied to multilayer adsorption process and is given by:

$$\text{Log} \frac{q_e}{q_e} = \text{Log} K_f + 1/n \text{ Log } C_e \quad \text{----- (4)}$$

Where,  $K_f$  is the Freundlich constant correspond to adsorption capacity (mg/L);  $n$  is a dimensionless constant related to the intensity of adsorption. The value of  $n$  reflects the degree of nonlinearity between adsorption process and concentration of dye. Values of  $K_f$  and  $n$  respectively are obtained from intercept and slope of the linear plot of  $\text{Log } q_e$  versus  $\text{Log } C_e$  (Fig.9).

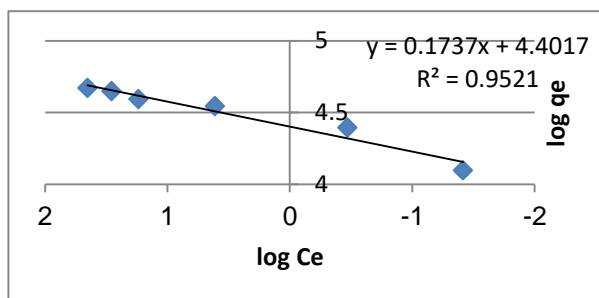


Fig 9 . Freundlich isotherm of adsorption of E102 dye on nanocomposite adsorbent

From the results which presented in table 3, the  $R^2$  value of Langmuir isotherm (0.99) was greater than that estimated from Freundlich (0.95) which reveal well fitted of adsorption isotherm with Langmuir equation. This result suggests that the adsorption of E102 dye by the nanocomposite is a homogeneous monolayer adsorption [25].

Table 3: Equilibrium adsorption parameters for Langmuir and Freundlich isotherm.

Estimated values of Langmuir equation			Estimated values of Freundlich equation		
$R^2$	$q_{\text{max}}$ (mg/g)	$K_L$ (Lmg <sup>-1</sup> )	$R^2$	$K_f$ (Lmg <sup>-1</sup> )*10 <sup>3</sup>	$n$
0.99	5*10 <sup>6</sup>	0.01	0.95	25.11886	5.757

### 3.4. Kinetics of Adsorption

Many kinetics models were applied to study the mechanism of dye adsorption process on the surface of adsorbents. The most widely used kinetic models, are Lagergren-first-order equation, and pseudo-second-order equation. These equations have been used to study the adsorption kinetic behavior of E102 dye (40 mg/l) onto nanocomposite at 45°C (optimum conditions). The best fit model was selected based on the linear regression correlation coefficient values ( $R^2$ ).

The linear form of the pseudo-first order kinetic [26] can be give as follows:

$$\log(q_e - q_t) = \log q_e - (k_1/2.303) t \quad \text{----- (5)}$$

where  $k_1$  is the rate constant of the pseudo-first order kinetics (min<sup>-1</sup>),  $q_e$  is the amount of E102 dye adsorbed on the surface of nanocomposite at equilibrium,  $q_t$  is the amount of E102 dye adsorbed on the surface of nanocomposite at any time. The  $q_e$  and  $k_1$  are calculated from the intercept and the slope of plots of  $\log(q_e - q_t)$  vs  $t$ , respectively. The result of such plot is illustrated in (fig. 10).

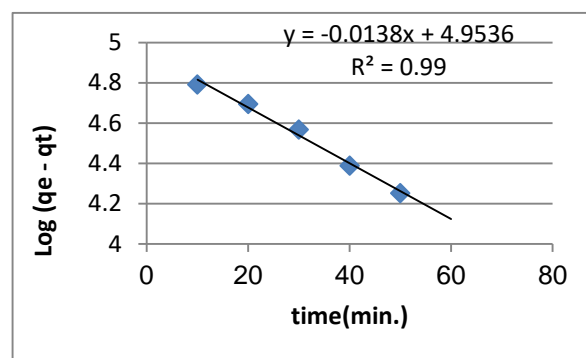


Fig 10. Pseudo first order plot of kinetics adsorption of E102 dye on nanocomposite at 45°C.

The linear form of the pseudo-second order kinetic model [27] is given as follows:

$$\frac{t}{q_t} = \frac{1}{k_2 q_e^2} + \left(\frac{1}{q_e}\right) t \quad \dots \dots \dots (6)$$

Where  $k_2$  is the rate constant (g mg<sup>-1</sup> min<sup>-1</sup>) of the pseudo-second order kinetics. From the intercept and the slope of  $t / q_t$  plots against  $t$ , respectively,  $k_2$  and  $q_e$  are calculated as shown in (Fig. 11).

From the kinetics parameters in Table 4, the values of correlation coefficients of the two equation (0.99 for first order and 1 for second order) are closely even the value of  $R^2$  of pseudo second order equation is slightly higher. This means that pseudo second order kinetics equation gave well-fitting with adsorption kinetics data. schematic of dye adsorption has been depicted in figure(12).

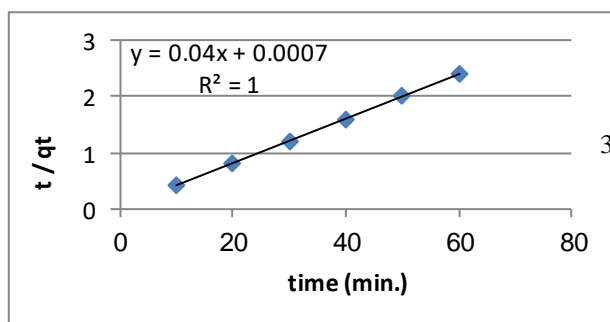


Fig 11. Pseudo second order plot of kinetics adsorption of E102 dye on nanocomposite at 45°C

Table 4: Kinetics parameters of adsorption of E102 dye on nanocomposite adsorbent.

Kinetics equations	R2	k	qe (mg/g)
Pseudo First order	0.99	0.0317(min <sup>-1</sup> )	89.125*10 <sup>3</sup>
Pseudo Second order	1	0.437 (g mg <sup>-1</sup> min <sup>-1</sup> )	25

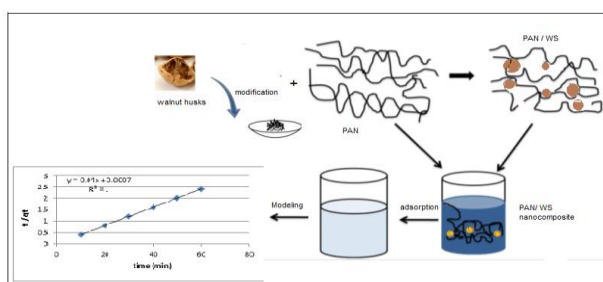


Fig 12. Schematic representation of dye adsorption.

#### 4. Conclusions

New, cheap and ecofriendly sample of nanocomposite was developed for removal pollutant dyes from wastewater. E102 dye was selected to study the adsorptive efficiency of the prepared sample of nanocomposite. Different factors were studied to get optimum conditions of adsorption E102 dye on nanocomposite surface and the results were 0.08 g of NC/50 ml of solution and 60 min contact time to reach equilibrium which reveal highly efficient of nanocomposite as adsorbent. Equilibrium parameters show best fitted with Langmuir model. According to their correlation coefficient, both kinetics equations (pseudo first and pseudo second order reaction) fitted with the results of adsorption rate, but second order equation gave better fitness.

#### 5. References

- Zoia PAHOM, Florina Branzoi, Gheorghe Nechifor, Electrochemical behaviour of new polymer composite coatings on carbon steel in acid medium, U.P.B. Sci. Bull., Series B, Vol. 80, Iss. 3, ISSN 1454-2331(2018).

- TAHA N.A., EL-MAGHRABY A., Magnetic peanut hulls for methylene blue dye removal :Isotherm and kinetic study. Global NEST journal ,vol.18(1),pp.24-36,(2016).
- RuihuaHuang·QianLiu·JieHuo·BingchaoYang., Adsorption of methyl orange onto protonated cross-linked chitosan.Arabian Journal of Chemistry,Volume 10, Issue 1, Pages 24-32,(2017).
- Shixiong Sheng, Bo Liu , Xiangyu Hou, Bing Wu, Fang Yao, Xinchun Ding and Lin Huang. Aerobic Biodegradation Characteristic of Different Water-Soluble Azo Dyes. Int. J. Environ. Res. Public Health, 15, 35;(2018) doi:10.3390/ijerph15010035 pp.1-11.
- SyieluingWong.,Hasnaa H.Tumari.,NorzitaNgadi.,Nurul BalqisMohamed.,OnnHassanRamliMat.,Nor AishahSaidina Amin.,Adsorption of anionic dyes on spent tea leaves modified with polyethyleneimine (PEI-STL). Journal of Cleaner Production,Volume 206, Pages 394-406,(2019).
- H. Eisazadeh and B. G. Bistouni, Korean J. Chem. Eng., 28, 287 ,(2011).
- Yagub ,M.T.,Sen,T.K.,Afroze,S.,Ang,H.M., Dye and its removal from aqueous Solution by adsorption :a review. Adv. Colloid interface Sci.209,172-184,(2014).
- Nazari, G., Abolghasemi, H., Esmaili, M. Batch adsorption of cephalexin antibiotic from queous solution by walnut shell-based activated carbon. Journal of the Taiwan Institute of Chemical Engineers, 58, 357–365.(2016).
- Salvatore Cataldo,Antonio Gianguzza,Demetrio Milea,Nicola Muratore,Alberto Pettignano & Silvio Sammartano. A critical approach to the toxic metal ion removal by hazelnut and almond shells. *Environmental Science and Pollution Research* **volume 25**, pages4238–4253(2018).
- Zou, Z., Tang, Y., Jiang, C., Zhang, J. Efficient adsorption of Cr(VI) on sunflower seed hull derived porous carbon. Journal of Environmental Chemical Engineering, 3(2), 898–905.(2015).
- Foo, K.Y., Hameed, B.H. Mesoporous activated carbon from wood sawdust by K<sub>2</sub>CO<sub>3</sub> activation using microwave heating. Bioresource Technology, 111, 425–432.(2012a).
- Foo, K.Y., Hameed, B.H. Preparation, characterization and evaluation of adsorptive properties of orange peel based activated carbon via microwave induced K<sub>2</sub>CO<sub>3</sub> activation. Bioresource Technology 686-679,104,(2012b).
- Ayad, M.M., El-Nasr, A.A. Adsorption of cationic dye (methylene blue) from water using polyaniline nanotubes base. Journal of Physical Chemistry C, 114(34), 14377–14383.(2010).
- SushmitaBanerjeeM.C.Chattopadhyaya. Adsorption characteristics for the removal of a toxic dye, tartrazine from aqueous solutions by a low cost agricultural by-

- product)Arabian.j.of chemistry,vol .10,page :S1629-S1638.(2017).
15. 15. Yusef Omidi Khaniabadi, Mohammad Javad Mohammadi, Mojtaba Shegerd,Shahram Sadeghi,Sedigheh Saeedi, Removal of Congo red dye from aqueous solutions by a low-cost adsorbent: activated carbon prepared from Aloe vera leaves shell. *Environmental Health Engineering and Management Journal*, 4(1), 29–35.(2017).
  16. 16.Sujata Saxena and A. S. M. Raja , Natural Dyes: Sources, Chemistry,Application and Sustainability Issues .S. S. Muthu (ed.), Roadmap to Sustainable Textiles and Clothing,Textile Science and Clothing Technology, DOI: 10.1007/978-981-287-065-0\_2, Springer Science+Business Media Singapore .pp.38.(2014).
  17. Viswanathan B. Photocatalytic Degradation of Dyes: An Overview. *Current Catalysis*, 7(1)99-121.(2018).
  18. Darvishmanesh S., Pethica B.A., Sundaresan S. Forward osmosis using draw solutions manifesting liquid-liquid phase Separation. *Desalination*. ;421:23–31,(2017).
  19. Khan A. M., Khan I. M., Zafar S. Removal of different anionic dyes from aqueous solution by anion exchange membrane. *Membrane water treatment*. 8(3) 259-277.(2017).
  20. Shena J., Shahida S., Amuraa I., Sarihana A., Tiana M., Emanuelsson E.A. Enhanced adsorption of cationic and anionic dyes from aqueous solutions by polyacid doped polyaniline. *Synth. Met.* ;245:151–159.(2018).
  21. L. Shi, X. Wang, L. Lu, X. Yang, X. Wu, Preparation of TiO<sub>2</sub>/polyaniline nanocomposite from a lyotropic liquid crystalline solution, *Synthetic Metals* 159 ,2525–2529. (2009) .
  22. 22. Di Zhang, Huaiyin Chen, and Ruoyu Hong, Preparation and Conductive and Electromagnetic Properties of Fe<sub>3</sub>O<sub>4</sub>/PANI Nanocomposite via Reverse In Situ Polymerization.*Journal of nanomaterials*, Volume 2019 |Article ID 7962754 | <https://doi.org/10.1155/2019/7962754>.
  23. 23.SushmitaBanerjeeM.C.Chattopadhyaya(Adsorption characteristics for the removal of a toxic dye, tartrazine from aqueous solutions by a low cost agricultural by-product)Arabian.j.of chemistry,vol .10,page :S1629-S1638.(2017).
  24. Ionela-Gabriela BACIOIU, Carolina Constantin,Ana-MariaStanescu, Ligia Stoica, Removal of Tartrazine (E102) From aqueous solutions by sorption – flotation ,U.P.B. Sci. Bull., Series B, Vol.78, Iss.1, ISSN 1454-2331(2016).
  25. Ayawei N., Ebelegi A.N., Wankasi D. Modelling and interpretation of adsorption isotherms. *J. Chem.* (2017):3039817. doi: 10.1155/2017/3039817. [CrossRef] [Google Scholar] [Ref list].
  26. Lagergren, S.. For the theory so-called adsorption of dissolved substances. *Kungliga Svenska Vetenskapsakademiens Handlingar*. ;24(4):1-39.(1898).
  27. Jean-Pierre Simonin., On the comparison of pseudo-first order and pseudo-second order rate laws in the modeling of adsorption kinetics.*Chem. Eng. J.*, (2016) DOI: <http://dx.doi.org/10.1016/j.cej.2016.04.079>.